

Event-Triggered Polynomial Control for Trajectory Tracking of Unicycle Robots

Anusree Rajan¹, Harini V², Bharadwaj Amrutur², and Pavankumar Tallapragada^{1,2}

Abstract—This paper proposes an event-triggered polynomial control method for trajectory tracking of unicycle robots. In this control method, each control input signal between two consecutive events is a polynomial. At each event, the coefficients of the polynomial control input are chosen to minimize the error in approximating a continuous-time control signal. We design an event-triggering rule that guarantees uniform ultimate boundedness of the tracking error. We ensure the absence of zeno behavior by showing the existence of a uniform positive lower bound on the inter-event times. We illustrate our results through numerical simulations and experiments. We show that the number of events generated by the proposed controller is significantly less compared to a time-triggered controller and an event-triggered controller based on zero-order hold, while guaranteeing similar tracking performance.

Index Terms—Networked control systems, event-triggered control, trajectory tracking

I. INTRODUCTION

Trajectory tracking for mobile robots is a well-studied problem with many applications, such as industrial automation, military surveillance and multi-robot coordination. An important challenge in these applications is constrained resources, such as communication, computation, and energy. Event-triggered control [1]–[4] is a popular method for control under such resource constraints. In the event-triggered control literature, design of control laws is mostly based on the zero-order-hold (ZOH) technique. However, there is a minimum packet size for many of the communication protocols used in control applications, such as TCP and UDP [5]. ZOH control may therefore result in under utilization of each packet while simultaneously increasing the number of communication instances. On the other hand, the use of non-ZOH control could improve the utilization of each packet while reducing the number of communication instances. With these motivations, in this paper, we propose an event-triggered polynomial control method for trajectory tracking of unicycle robots.

A. Literature Review

The literature on trajectory tracking with event-triggered communication is limited. Reference [6] designs an event-triggered tracking controller for non-linear systems that guarantees uniform ultimate boundedness of the tracking error and non-zeno behavior of inter-event times. Similarly, references [7]–[9] propose Lyapunov based event or self-triggered

tracking controllers for mobile robots by emulating a continuous time controller and guarantee ultimate boundedness of the tracking error. Reference [10] obtains a linear system model for a Pioneer robot by system identification and designs an adaptive self-triggered tracking controller. Reference [11] proposes an event-triggered optimal tracking control method for nonlinear systems using ideas from reinforcement learning. Whereas, reference [12] presents a self-triggered model predictive control strategy for trajectory tracking of unicycle-type robots with input constraints and bounded disturbances. Reference [13] deals with the tracking control of quadrotors with external disturbances and proposes an event-triggered sliding mode control strategy. The recent paper [14] proposes both event-triggered and self-triggered saturated feedback control strategies for trajectory tracking of unicycle mobile robots. In all these papers, the control input to the plant is held constant between two successive events.

There are a limited number of works on non-ZOH event-triggered control. Among them is the idea of model-based event-triggered control [15]–[18]. In this method the control input to the plant is time-varying even between two successive events and is generated using a model of the plant. Essentially, both the controller and the actuator have identical copies of the model and synchronously update the state of the model in an event-triggered manner. For this reason, the method is mainly used in control of linear systems. Another method based on non-ZOH is event-triggered dead-beat control [19]. In this method, the controller transmits a sequence of control inputs to the actuator at each triggering instant over communication channel. This control sequence is stored in a buffer and applied sequentially to the plant until the next control packet arrives. References [20], [21] extend the idea of deadbeat control in that the actuator applies the control input to the plant based on first-order-hold (FOH) between the control sequence until it receives a new sequence at the next triggering instant. In our recent work [22], we propose an event-triggered parameterized control method for stabilization of linear systems.

B. Contributions

The main contribution of this work is that we propose an event-triggered polynomial control method for trajectory tracking of unicycle robots where the reference trajectory is modeled as the solution of a reference system with unicycle dynamics. In this control method, between two consecutive events, each control input to the robot is a polynomial whose coefficients are chosen to minimize the error in approximating a continuous-time control signal. At each event, the coefficients of the polynomial control input are computed and

¹ Department of Electrical Engineering, Indian Institute of Science

² Robert Bosch Centre for Cyber Physical Systems, Indian Institute of Science

{anusreerajan, hariniv, amrutur, pavant}@iisc.ac.in

communicated to the actuator. The proposed event-triggered controller guarantees uniform ultimate boundedness of tracking error and non-zero behavior of inter-event times. The proposed method works best in cases where communication is significantly more costly than computation.

Our method generalizes the ZOH and FOH-based event-triggered control techniques. Our technique can be fine-tuned to utilize the whole payload per packet of communication and, as a result, also requires fewer communication instances or packets than ZOH or FOH control. In model-based event-triggered control method, the actuator must have sufficient computing power to simulate the system model online. This may be extremely challenging if the system is nonlinear or the control task is complex. Additionally, both at the controller and the actuator, the state of the model must be updated simultaneously. This can be problematic if there are unidentified time delays in the communications. Furthermore, sharing a copy of the system model at the actuator is highly unfavourable from a privacy and security perspective. In order to achieve the same level of approximation of an ideal control signal as provided by our proposed polynomial control strategy, methods like event-triggered control based on FOH or deadbeat control require a large number of samples to be transmitted at each event. This is because, regardless of the length of the signal, our method only requires a limited number of parameters to be communicated. Moreover, the literature on event-triggered model-based control, deadbeat control, or control based on FOH mostly deals with stabilization problems, while tracking control problems are less addressed. The only paper that considers a control method similar to the one proposed is [22], where an event-triggered parametrized control method is proposed for stabilization of linear systems. On the other hand, in the current paper, the context is trajectory tracking for unicycle robot models. Finally, even now, the number of papers that carry out practical experiments of event-triggered controllers is quite small. Thus, the experimental results in this paper are also a major contribution.

C. Organization

Section II formally presents the system dynamics and the objective of this paper. In Section III, we design a polynomial control law and an event-triggering rule to achieve our objective. Then, in Section IV, we analyze the proposed controller and show uniform ultimate boundedness of tracking error as well as non-Zeno behavior of inter-event times. Section V illustrates the results through simulations and experiments. Finally, we provide some concluding remarks in Section VI.

D. Notation

Let \mathbb{R} and \mathbb{R}^n denote the set of real numbers and n -dimensional real vector space, respectively. Let \mathbb{N} and \mathbb{N}_0 denote the set of all positive and non-negative integers, respectively. For any $x \in \mathbb{R}^n$, $\|x\|$ denotes the euclidean norm of x . For an $n \times m$ matrix B , let B_i denote the i^{th} row of B . For any two functions $v, w : [0, T] \rightarrow \mathbb{R}$, let

$$\langle v, w \rangle := \int_0^T v(\tau)w(\tau)d\tau.$$

II. PROBLEM SETUP

In this paper, we propose a tracking control method that works best in cases where communication is significantly more costly than computation. In this section, we present the system dynamics and the objective of this paper.

A. System Dynamics

Consider a unicycle robot modeled as follows,

$$\dot{x} = v \cos \theta, \quad \dot{y} = v \sin \theta, \quad \dot{\theta} = \omega, \quad (1)$$

where (x, y) denotes the position of the robot and θ denotes the orientation of the robot, which is the angle between the heading direction of the robot and the x -axis. v and ω denote, respectively, the linear velocity and the angular velocity of the robot, which are the control inputs. The position and the orientation of the robot are continuously available to the controller.

The robot has to track a given reference trajectory which satisfies the following dynamics,

$$\dot{x}_r = v_r \cos \theta_r, \quad \dot{y}_r = v_r \sin \theta_r, \quad \dot{\theta}_r = \omega_r, \quad (2)$$

where (x_r, y_r) and θ_r denote, respectively, the reference position and the reference orientation. v_r and ω_r denote the inputs to the reference system. We make the following assumption on the reference inputs, just as in [7].

(A1) There exists $M \geq 0$ such that $|v_r(t)|, |\omega_r(t)|, |\dot{v}_r(t)|$ and $|\dot{\omega}_r(t)|$ are upper bounded by M , $\forall t \geq t_0$. Moreover, there exists a $c > 0$ such that $|v_r(t)| \geq c$, $\forall t \geq t_0$. •

We also assume that the reference trajectory and the reference inputs are available to the controller a priori.

The tracking error, in the robot frame, can be represented as follows,

$$\begin{bmatrix} x_e \\ y_e \\ \theta_e \end{bmatrix} := \begin{bmatrix} \cos \theta & \sin \theta & 0 \\ -\sin \theta & \cos \theta & 0 \\ 0 & 0 & 1 \end{bmatrix} \begin{bmatrix} x_r - x \\ y_r - y \\ \theta_r - \theta \end{bmatrix}, \quad (3)$$

which we can re-express as

$$\dot{X} = F(X, t) + G(X)u, \quad (4)$$

where $X = [x_e \quad y_e \quad \theta_e]^T$, $u = [v \quad \omega]^T$,

$$F(X, t) = [v_r \cos \theta_e \quad v_r \sin \theta_e \quad \omega_r]^T,$$

$$G(X) = \begin{bmatrix} -1 & y_e \\ 0 & -x_e \\ 0 & -1 \end{bmatrix}.$$

We consider a polynomial control input whose coefficients are updated in an event-triggered manner. In other words, each control input to the plant is a polynomial of degree p during the time between any two consecutive events. Now, let $u_1(t) := v(t)$ and $u_2(t) := \omega(t)$. Then, for $i \in \{1, 2\}$,

$$u_i(t_k + \tau) = f(\mathbf{a}_i(k), \tau) := \sum_{j=0}^p a_{ji}(k) \tau^j, \quad \forall \tau \in [0, t_{k+1} - t_k]. \quad (5)$$

Here $(t_k)_{k \in \mathbb{N}_0}$ is the sequence of communication time instants from the controller to the actuator. At t_k , the controller

communicates the coefficients of the polynomial control input, $\mathbf{a}(k) := [a_{ji}(k)] \in \mathbb{R}^{(p+1) \times 2}$, to the actuator. We also let $\mathbf{a}_i(k)$ denote the i^{th} column of $\mathbf{a}(k)$. Note that, in contrast to the usual trend in event-triggered control literature, here the control input to the robot is not held constant between two communication time instants.

B. Objective

Our objective is to design a polynomial control law and an event-triggering rule to implicitly determine the communication time instants $(t_k)_{k \in \mathbb{N}_0}$, at which the coefficients of the polynomial control input are updated, so that the tracking error is uniformly ultimately bounded. We also wish to ensure the existence of a uniform positive lower bound on the inter-event times.

III. DESIGN OF THE EVENT-TRIGGERED CONTROLLER

In this section, we design a polynomial control law as well as an event-triggering rule to achieve our objective.

A. Control Law

We first consider the continuous time feedback control signal, $\hat{u} := [\hat{v} \quad \hat{\omega}]^T$, that was proposed in [23]. In particular,

$$\begin{aligned} \hat{v}(\hat{X}, t) &= v_1 + c_1(\hat{x}_e - c_3 \hat{\omega}(\hat{X}, t) \hat{y}_e), \\ \hat{\omega}(\hat{X}, t) &= \omega_r + \gamma \hat{y}_e v_r \text{sinc}' \hat{\theta}_e + c_2 \gamma \hat{\theta}_e, \end{aligned} \quad (6)$$

where

$$\begin{aligned} v_1 &= v_r \cos \hat{\theta}_e - c_3 v_2 \hat{y}_e + c_3 \hat{\omega}(\hat{X}, t) (\hat{\omega}(\hat{X}, t) \hat{x}_e - v_r \sin \hat{\theta}_e), \\ v_2 &= \hat{\omega}_r + \gamma v_r \text{sinc}' \hat{\theta}_e (-\hat{\omega}(\hat{X}, t) \hat{x}_e + v_r \sin \hat{\theta}_e) + \gamma \hat{y}_e v_r \text{sinc}' \hat{\theta}_e \\ &\quad + (\gamma \hat{y}_e v_r \text{sinc}' \hat{\theta}_e + c_2 \gamma) (\omega_r - \hat{\omega}(\hat{X}, t)). \end{aligned} \quad (7)$$

Here $\hat{X} := [\hat{x}_e \quad \hat{y}_e \quad \hat{\theta}_e]^T$ follows the dynamics,

$$\dot{\hat{X}} = F(\hat{X}, t) + G(\hat{X}) \hat{u}(\hat{X}, t), \quad \forall t \in [t_k, t_{k+1}), \quad (8)$$

where $\hat{X}(t_k) = X(t_k)$ for all $k \in \mathbb{N}_0$. Note also that $\text{sinc}' \hat{\theta}_e$ denotes the derivative of $\text{sinc} \hat{\theta}_e$ with respect to $\hat{\theta}_e$ and $c_1, c_2, c_3, \gamma > 0$ are design parameters. Reference [23] considers the tracking error dynamics (4) with $u = \hat{u}(X, t)$ and shows global convergence of tracking error to zero under some conditions on the reference inputs.

Our idea is to find the best polynomial approximation of the control signal (6). At each communication time instant t_k , the coefficients of the polynomial control input (5) are updated by solving the following finite horizon optimization problems, for $i \in \{1, 2\}$,

$$\begin{aligned} \mathbf{a}_i(k) &= \arg \min_{a \in \mathbb{R}^{p+1}} \int_0^T [|f(a, \tau) - \hat{u}_i(\hat{X}, t_k + \tau)|^2 + \delta_i |f(a, \tau)|^2] d\tau, \\ \text{s.t. } f(a, 0) &= \hat{u}_i(\hat{X}(t_k), t_k), \end{aligned} \quad (9)$$

where $\hat{u}_1 := \hat{v}$ and $\hat{u}_2 := \hat{\omega}$. Here, $T > 0$ is a finite time horizon which is to be designed and $\delta_1, \delta_2 \geq 0$ are design parameters which are useful for penalizing large magnitudes of the control input signal. Note that, in order to solve the optimization

problem (9), we require the values of \hat{v} and $\hat{\omega}$ over the time horizon $(t_k, t_k + T]$. These values are estimated by numerically simulating the system (8).

Note that, the only constraint in optimization problem (9) fixes the value of a_0 . Hence, letting

$$\bar{u}_i(\tau) := \hat{u}_i(\hat{X}, t_k + \tau), \quad \mu_i := \bar{u}_i(0),$$

we can rewrite (9) as the following unconstrained optimization problem, for $i \in \{1, 2\}$,

$$\bar{\mathbf{a}}_i(k) = \arg \min_{a \in \mathbb{R}^p} J_i(a), \quad (10)$$

where,

$$\begin{aligned} J_i(a) &= \langle \bar{u}_i, \bar{u}_i \rangle + (1 + \delta_i) \mu_i^2 T - 2 \mu_i \langle \bar{u}_i, 1 \rangle - 2 \sum_{j=1}^p a_j \langle \bar{u}_i, \tau^j \rangle \\ &\quad + (1 + \delta_i) \sum_{j=1}^p \left[\sum_{l=1}^p a_j a_l \frac{T^{j+l+1}}{j+l+1} + 2 \mu_i a_j \frac{T^{j+1}}{j+1} \right]. \end{aligned}$$

Thus, we have

$$\mathbf{a}_i(k) = [\mu_i \quad \bar{\mathbf{a}}_i^T(k)]^T.$$

Remark 1. (Control signal for $\tau > T$). Given the coefficients of the polynomial control input that are obtained by solving (10), the control input that is applied by the actuator is as given in (5). However, since t_k 's are implicitly determined by an event-triggering rule online, it may happen that $t_{k+1} - t_k > T$. In that case, we simply extend the control input $u(t_k + \tau)$ for τ beyond T by suitably extending the domain of the polynomial function f . •

Proposition 2. The optimization problem (10) is a convex optimization problem.

Proof. Let us show that the objective function of (10), $J_i(a)$, is convex in the optimization variable a for all $i \in \{1, 2\}$. The Hessian matrix of $J_i(\cdot)$, denoted as \mathbf{H}_i , is as follows,

$$\mathbf{H}_i = 2(1 + \delta_i) \begin{bmatrix} \frac{T^3}{3} & \frac{T^4}{4} & \cdots & \frac{T^{p+2}}{p+2} \\ \frac{T^4}{4} & \frac{T^5}{5} & \cdots & \frac{T^{p+3}}{p+3} \\ \cdots & \cdots & \cdots & \cdots \\ \frac{T^{p+2}}{p+2} & \frac{T^{p+3}}{p+3} & \cdots & \frac{T^{2p+1}}{2p+1} \end{bmatrix}, \quad \forall i \in \{1, 2\}.$$

Observe that \mathbf{H}_i is $2(1 + \delta_i)$ times the Gram matrix for the functions in $\{\tau^j : [0, T] \rightarrow \mathbb{R}\}_{j=1}^p$. Thus, \mathbf{H}_i is a positive semi-definite matrix $\forall i \in \{1, 2\}$. Hence, the cost function in (10) is convex. As there are no constraints in (10), it is a convex optimization problem. □

B. Event-Triggering Rule

We consider the candidate Lyapunov function,

$$V(X, t) = \frac{1}{2} x_1^2 + \frac{1}{2} y_e^2 + \frac{1}{2\gamma} \theta_e^2, \quad (11)$$

where $x_1 = x_e - c_3 \hat{\omega}(X, t) y_e$, to design the event-triggering rule. Please note that in x_1 , it is indeed $\hat{\omega}(X, t)$ and not $\hat{\omega}(\hat{X}, t)$. Letting

$$e(t) := u(t) - \hat{u}(X, t),$$

we see that the derivative of V along the trajectories of the sampled data system (4)-(5) can be expressed as

$$\begin{aligned}\dot{V} &= \frac{\partial V}{\partial t} + \frac{\partial V}{\partial X} \dot{X} = \frac{\partial V}{\partial t} + \frac{\partial V}{\partial X} (F(X,t) + G(X)u) \\ &= \frac{\partial V}{\partial t} + \frac{\partial V}{\partial X} (F(X,t) + G(X)(\hat{u}(X,t) + e(t))) \\ &= -\Sigma(X,t) + \Lambda(X,e,t)\end{aligned}\quad (12)$$

where

$$\Sigma(X,t) := c_1 x_1^2 + c_2 \theta_e^2 + c_3 \omega^2(X,t) y_e^2, \quad (13)$$

$$\Lambda(X,e,t) := \frac{\partial V}{\partial X} G(X) e(t). \quad (14)$$

The last equation in (12) follows directly from equation (41) in [23]. Note that, whenever an event occurs $\dot{V} = -\Sigma(X,t)$ as $e = 0$.

Now, we define the event-triggering rule as follows,

$$t_{k+1} := \min\{t > t_k : \dot{V} \geq -\sigma \Sigma(X,t) \text{ and } V(X,t) \geq \varepsilon^2\}, \quad (15)$$

where $t_0 := 0$ and $\sigma \in (0,1)$, $\varepsilon^2 > 0$ are design parameters.

In summary, the complete system, \mathcal{S} , is the combination of the reference system (2), the unicycle robot dynamics (4), the polynomial control law (5), with coefficients chosen by solving (10), which are updated at the events determined by the event-triggering rule (15). That is,

$$\mathcal{S} : (2), (4), (5), (10), (15). \quad (16)$$

IV. ANALYSIS OF THE EVENT-TRIGGERED CONTROL SYSTEM

In this section, we analyze the performance of the designed event-triggered control system. We show that for the complete system (16), the tracking error is uniformly ultimately bounded and the inter-event times have a uniform positive lower bound. We first present a lemma that helps to prove the main result of this paper.

Lemma 3. *Consider system (16) and Lyapunov function (11). Let Assumption (AI) hold and $\varepsilon_k^2 := V(X(t_k), t_k)$. Then, for any $c_1, c_2, c_3, \varepsilon^2 > 0$ and $\gamma > 0$ sufficiently large, $V(X(t), t) \leq \varepsilon_k^2, \forall t \in [t_k, t_{k+1})$ and $\forall k \in \mathbb{N}$.*

Proof. Let us prove this result by contradiction. Suppose that the result is not true. Then, as $V(X,t)$ is a continuous function of time, there must exist $\bar{t} \in [t_k, t_{k+1})$, for some $k \in \mathbb{N}$, such that $V(X(\bar{t}), \bar{t}) = \varepsilon_k^2$ and $\dot{V}(X(\bar{t}), \bar{t}) > 0$. However, the event-triggering rule (15) implies that $\varepsilon_k^2 \geq \varepsilon^2$ and $\dot{V}(X(\bar{t}), \bar{t}) < -\sigma \Sigma(X(\bar{t}), \bar{t}) < 0$. The last inequality follows from Lemma 4 in [7], which states that there exists $\mathcal{V} > 0$ for any $c_1, c_2, c_3, \varepsilon^2 > 0$ and $\gamma > 0$ sufficiently large such that $V(X,t) \geq \varepsilon^2$ implies $\Sigma(X,t) \geq \mathcal{V} > 0$. As there is a contradiction, we conclude that there does not exist such a \bar{t} and hence the result is true. \square

Remark 4. *Under Assumption (AI), $V(X,t)$, defined as in (11), is a continuous positive definite radially unbounded function of X .*

Next, we present the main theorem of this paper that shows that the inter-event times are uniformly lower bounded by

a positive real number and the tracking error is uniformly ultimately bounded.

Theorem 5. *(Absence of zeno behavior and uniform ultimate boundedness of tracking error). Consider system (16). Suppose Assumption (AI) holds. Then,*

- the inter-event times, $t_{k+1} - t_k$ for $k \in \mathbb{N}$, are uniformly lower bounded by a positive real number that depends on the bound of the initial tracking error.
- moreover, the lower bound on the inter-event times converges to a positive real number, which is independent of the initial tracking error, in finite time.
- the tracking error is uniformly ultimately bounded.

Proof. Let us first prove the first statement of this theorem. Note that, for each $k \in \mathbb{N}$, $\dot{V}(X(t_k), t_k) = -\Sigma(X(t_k), t_k)$. Hence, for each $k \in \mathbb{N}$, the inter-event time $t_{k+1} - t_k$ must be greater than the time it takes $\Lambda(X,e,t)$ to grow from 0 to $(1-\sigma)\Sigma(X,t)$.

Let $\varepsilon_k^2 := V(X(t_k), t_k)$. Given Lemma 3 and (14), we can find an upper bound on $\Lambda(X,e,t)$ as follows,

$$\Lambda(X,e,t) \leq L(\varepsilon_k^2) \|e\|, \quad \forall t \in [t_k, t_{k+1}),$$

where $L: \mathbb{R}_{>0} \rightarrow \mathbb{R}_{>0}$ is a continuous function defined as,

$$L(R) \geq \max_{V \leq R} \left\| \frac{\partial V}{\partial X} G(X) \right\|.$$

According to Remark 4, the right hand side of the above inequality exists as any sub-level set of V is compact. Also note that the event-triggering rule (15) implies that for each $k \in \mathbb{N}$, $V(X(t_k), t_k) \geq \varepsilon^2$. Hence, we can say that for any $k \in \mathbb{N}$, the inter-event time $t_{k+1} - t_k$ is lower bounded by the time it takes $\|e\|$ to grow from 0 to $(1-\sigma) \frac{\mathcal{V}}{L(\varepsilon_k^2)}$, where $\mathcal{V} > 0$ is the same constant mentioned in the proof of Lemma 3. Now, we make the following claim.

Claim (a): There exist monotonically increasing functions $\beta_1: \mathbb{R}_{>0} \rightarrow \mathbb{R}_{>0}$, $\beta_2: \mathbb{R}_{>0} \rightarrow \mathbb{R}_{>0}$ such that $\|u(t)\| \leq \beta_1(\varepsilon_k^2)$ and $\|\dot{u}(t)\| \leq \beta_2(\varepsilon_k^2)$, $\forall t \in [t_k, \min\{t_{k+1}, t_k + T\})$, $\forall k \in \mathbb{N}$.

Let us prove claim (a). Note that, $\forall i \in \{1, 2\}$ and for any $k \in \mathbb{N}$, $u_i(t)$ for $t \in [t_k, t_{k+1})$ is chosen by solving the unconstrained optimization problem (10), which we have seen in Proposition 2 is also convex.

Thus, the stationarity condition is necessary and sufficient. Thus, the optimizers of problem (10) are the solutions of

$$\mathbf{H}_i \bar{\mathbf{a}}_i(k) = D_i(k)$$

where \mathbf{H}_i is the Hessian matrix given in the proof of Proposition 2 and

$$D_i(k) = 2 \begin{bmatrix} \langle \bar{u}_i, \tau^1 \rangle \\ \langle \bar{u}_i, \tau^2 \rangle \\ \vdots \\ \langle \bar{u}_i, \tau^p \rangle \end{bmatrix} - 2(1 + \delta_i) \mu_i \begin{bmatrix} \frac{T^2}{2} \\ \frac{T^3}{3} \\ \vdots \\ \frac{T^{p+1}}{p+1} \end{bmatrix}.$$

Now, recall from the proof of Proposition 2 that \mathbf{H}_i is $2(1 + \delta_i)$ times the Gram matrix for the functions in $\{\tau^j: [0, T] \rightarrow \mathbb{R}\}_{j=1}^p$. Since these functions are linearly independent, we can

say that \mathbf{H}_i is invertible. So, there is a unique optimal solution $\bar{\mathbf{a}}_i(k)$ to the problem (10) and is equal to $\bar{\mathbf{a}}_i(k) = \mathbf{H}_i^{-1}D_i(k)$.

Now, note that, $V(\hat{X}(t), t) \leq V(\hat{X}(t_k), t_k)$ for all $t \in [t_k, \min\{t_{k+1}, t_k + T\})$ and for any $k \in \mathbb{N}$ as $\dot{V}(\hat{X}, t) = -\Sigma(\hat{X}, t) \leq 0$ where \hat{X} follows the dynamics (8). As $\hat{X}(t_k) = X(t_k)$, $V(\hat{X}(t_k), t_k) = V(X(t_k), t_k)$ for each $k \in \mathbb{N}$. According to Remark 4,

we can say that there exists a class \mathcal{K} function $\alpha'(\cdot) > 0$ such that $\|\hat{X}(t)\| \leq \alpha'(\varepsilon_k^2)$ for all $t \in [t_k, \min\{t_{k+1}, t_k + T\}]$ for each $k \in \mathbb{N}$. This implies that, for each $i \in \{1, 2\}$, for all $\tau \in [0, \min\{t_{k+1} - t_k, T\})$ and $\forall k \in \mathbb{N}$, $|\bar{u}_i(\tau)|$ is upper bounded by a monotonically increasing positive real valued function of ε_k^2 . By using this fact, we can say that there exists a monotonically increasing function $\beta'(\cdot)$ such that $\|\mathbf{a}(k)\| \leq \beta'(\varepsilon_k^2)$, $\forall k \in \mathbb{N}$. Thus, we can say that there exists monotonically increasing functions $\beta_1, \beta_2: \mathbb{R}_{>0} \rightarrow \mathbb{R}_{>0}$ such that $\forall t \in [t_k, \min\{t_{k+1}, t_k + T\})$, $\forall k \in \mathbb{N}$,

$$\|u(t)\| \leq \|\mathbf{a}(k)\| \left\| \begin{bmatrix} 1 \\ t - t_k \\ \vdots \\ (t - t_k)^p \end{bmatrix} \right\| \leq \beta_1(\varepsilon_k^2),$$

$$\|\dot{u}(t)\| \leq \|\mathbf{a}(k)\| \left\| \begin{bmatrix} 0 \\ 1 \\ \vdots \\ p(t - t_k)^{p-1} \end{bmatrix} \right\| \leq \beta_2(\varepsilon_k^2).$$

This proves claim (a).

Next, note that, $\hat{u}(X, t)$ is a continuously differentiable function of time. Thus, by using Lemma 3 and similar arguments as before, we can say that $\|\dot{\hat{u}}(X, t)\|$ is upper bounded by a monotonically increasing positive real valued function of ε_k^2 , $\forall t \in [t_k, t_{k+1})$, $\forall k \in \mathbb{N}$.

Then, $\forall t \in [t_k, \min\{t_k + T, t_{k+1}\})$, $\forall k \in \mathbb{N}$,

$$\frac{d}{dt} \|e(t)\| \leq \|\dot{e}(t)\| \leq \|\dot{u}(t)\| + \|\dot{\hat{u}}(X, t)\| \leq \alpha_e(\varepsilon_k^2),$$

for some monotonically increasing function $\alpha_e: \mathbb{R}_{>0} \rightarrow \mathbb{R}_{>0}$. Thus, for each $k \in \mathbb{N}$, the inter-event time $t_{k+1} - t_k$ is lower bounded by $(1 - \sigma) \frac{\nu}{\alpha_e(\varepsilon_k^2)L(\varepsilon_k^2)} > 0$.

Now, from Lemma 3, we know that $\varepsilon_1^2 \geq \varepsilon_k^2$, for $k \in \mathbb{N}$, where $\varepsilon_1^2 := V(X(t_1), t_1) \geq \varepsilon^2$. Hence, we can say that the inter-event times, for $k \in \mathbb{N}$, are uniformly lower bounded by $(1 - \sigma) \frac{\nu}{\alpha_e(\varepsilon_1^2)L(\varepsilon_1^2)} > 0$. This completes the proof of the first statement of this theorem. Next note that, according to Lemma 3 and the fact that the sequence of inter-event times does not exhibit zeno behavior, the event-triggering rule (15) implies that $\dot{V}(X(t), t) < -\sigma\Sigma(X(t), t) < 0$ for all $t \geq t_0$ such that $V(X(t), t) \geq \varepsilon^2$. Thus, there exists $\bar{t} \in [t_0, \infty)$ such that $V(X(t), t) \leq \varepsilon^2$ for all $t \geq \bar{t}$. Under Assumption (A1), this implies that the tracking error X is uniformly ultimately bounded. Moreover, we can also say that there exists a finite $\bar{k} \in \mathbb{N}$ such that $\varepsilon_k^2 = \varepsilon^2$ for all $k \geq \bar{k}$. Thus, the lower bound on the inter-event times converges to $(1 - \sigma) \frac{\nu}{\alpha_e(\varepsilon^2)L(\varepsilon^2)} > 0$ in finite time and events. This completes the proof of the last two statements of this theorem. \square

V. SIMULATION AND EXPERIMENTAL RESULTS

In this section, we present results of our simulations and experiments of the proposed event-triggered polynomial control (ETPC) for trajectory tracking. We compare the proposed method with time-triggered control (TTC) and the zero-order hold based event-triggered control algorithm described in [7], which we refer to as event-triggered control (ETC) here. We present the simulation and experimental results for four reference trajectories that were generated using the unicycle dynamics (2). The resulting paths in these four cases are shown in Figure 1. The reference velocity for these trajectories is 15cm/s. In paths 1 and 3, the reference angular velocity, ω_r is either constant or smoothly changing while in paths 2 and 4, ω_r is discontinuous at some time instants.

Evaluation metrics: Let T_e be the total simulation/experiment time duration. We define the transient period as the time interval $[0, T_c]$, where

$$T_c := \min\{t \geq 0 : V(t) \leq \varepsilon^2\},$$

that is T_c is the time the Lyapunov function V takes to converge to the ε^2 value. We define the steady state period as the time interval $(T_c, T_e]$. Let N_t and N_s be the total number of events in the transient and steady state periods, respectively.

We compare the proposed ETPC with ETC and TTC in terms of the number of events, N_t and N_s , and the convergence time T_c . In order to do a fair comparison with TTC, we compare ETC and ETPC against TTC with two different transmission frequencies/periods. In particular, henceforth, TTC1 and TTC2 refer to TTC with average transmission frequency over T_e for ETC and ETPC respectively, in the corresponding simulation or experiment.

In general, the ultimate bound of $V(t)$ for TTC1 and TTC2 is higher than ε^2 . In practical experiments with ETC and ETPC also the ultimate bound is often higher ε^2 . This is due to several unmodeled features, including sampling rate for the motion capture system (restricted to 240 frames per second here), measurement latency, error in obtained pose information, computation times for solving the optimization problem (9), communication delays and latency, delay introduced by onboard serial communication on robot, environmental conditions such as slip and non-uniform surface friction. Even the kinematics of the robot may not exactly be unicycle dynamics. Given all this, another evaluation metric we employ is $\varepsilon_1^2 \geq \varepsilon^2$, the ultimate bound for $V(t)$. Specifically, we define ε_1^2 as

$$\varepsilon_1^2 := \max_{t \geq T_c} \{V(t)\}.$$

A. Simulations

Simulations were done for the system (16) with four reference trajectories that generate the paths shown in Figure 1. In the simulations, the integration time step was a fixed value of 5ms for all the algorithms. The design parameters were chosen as $\gamma = 100$, $c_1 = 0.02$, $c_2 = 0.05$, $c_3 = 0.01$, $\sigma = 0.5$ and $\varepsilon = 0.1$. The prediction time horizon for ETPC, T was chosen as 1 second. The initial pose error was sampled uniformly from the set $[(-2\text{m}, 2\text{m}), (-2\text{m}, 2\text{m}), (-0.2\text{radians}, 0.2\text{radians})]$ to get a set of 1000 initial conditions. Simulations were

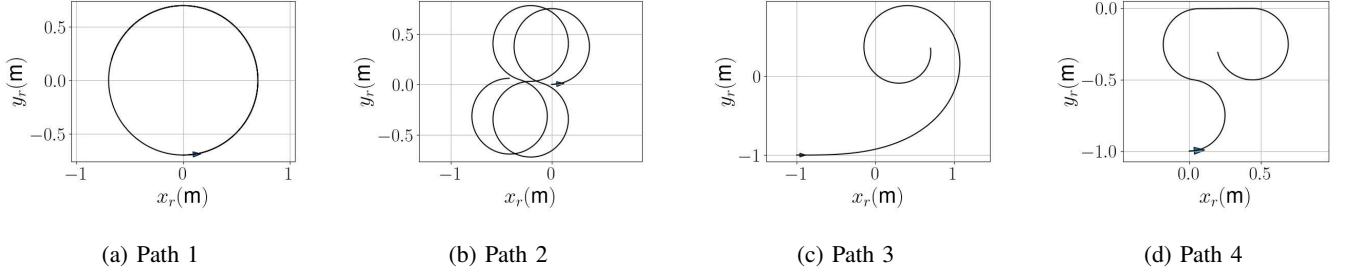


Fig. 1: Reference trajectories under consideration.

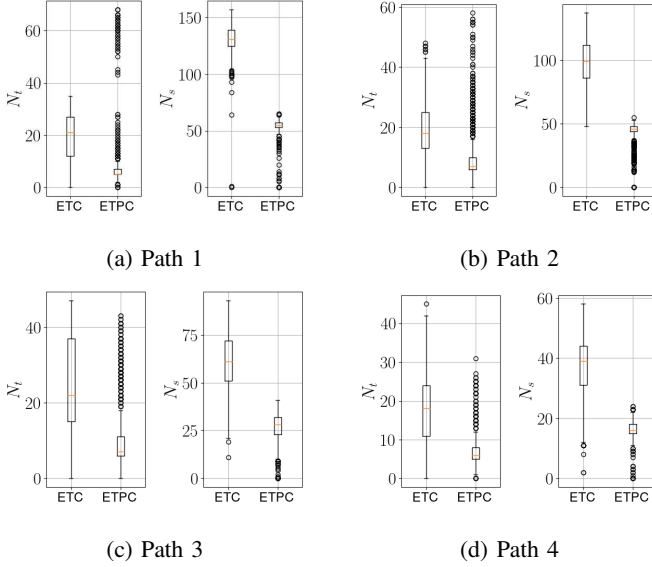


Fig. 2: Comparison of number of events for simulated paths for algorithms under consideration.

conducted for each algorithm, for each of the four paths in Figure 1, for each of these 1000 initial conditions. Figure 2 depicts the number of events for paths 1 to 4 in the transient and steady state period for ETC and ETPC. We compare the median values to quantify improvements. It is observed that the median of N_s for ETPC shown in Figure 2 is reduced by 70.3%, 62.7%, 67.3% and 77% in comparison to median of N_s for ETC for paths 1 to 4 respectively. Similarly, the median of N_t for ETPC is reduced by 38.1%, 38.9%, 22.8% and 38.9% in comparison to median of N_t for ETC for paths 1 to 4, respectively.

In all cases, the third quartile for ETPC is much lower than even the first quartile for ETC. Thus, we can say that the our algorithm requires far fewer number of events than ETC.

Figure 3 shows the ultimate bound of V for TTC1 and TTC2 algorithms for all the paths. The ultimate bound of V for ETC and ETPC is within numerical tolerance of ϵ^2 bound. The TTC1 and TTC2 algorithms often give an ultimate bound in the order of hundreds. Thus, we can conclude that the tracking performance with ETC or ETPC is significantly better than that of TTC with comparable frequency of transmissions.

Figure 4 shows the evolution of pose error under ETPC for Path 3 with the initial pose error $(-1.02 \text{ m}, 1.08 \text{ m}, 0.142 \text{ rad})$.

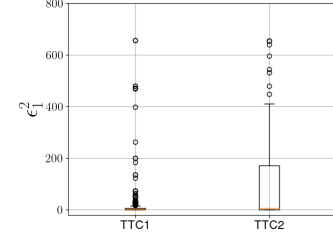


Fig. 3: Ultimate bound of V for all simulated paths using TTC1 and TTC2.

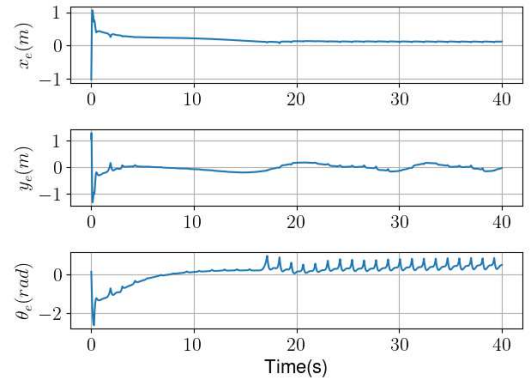


Fig. 4: Evolution of pose error for simulated Path 3 with initial pose error of $(-1.02 \text{ m}, 1.08 \text{ m}, 0.142 \text{ rad})$ with ETPC.

It is observed that the error reduces over time and then oscillates to ensure that V stays within ϵ^2 bound. Figure 5 shows the evolution of Lyapunov function for ETC and ETPC for Path 3 with the above initial pose error. It is observed that both ETC and ETPC stay within the ϵ^2 bound once they enter it. Notice that in Figure 4, θ_e oscillates significantly even at the end of the simulation. However the corresponding V stays within ϵ^2 bound once it enters it. This happens because the contribution of θ_e to V is reduced significantly by a factor of 200 as seen from (11).

B. Practical Experiments

The experiments have been conducted on a 3pi+ 32U4 robot manufactured by Pololu Robotics and Electronics [24]. The robot is equipped with two quadrature encoders which are utilized for robot level wheel velocity control done using a

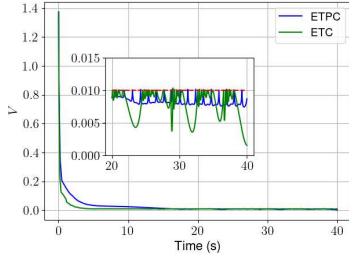


Fig. 5: Evolution of Lyapunov function for simulated Path 3 for initial pose error of $(-1.02 \text{ m}, 1.08 \text{ m}, 0.142 \text{ rad})$.

conventional PID controller. The microcontroller on the robot is an AtMega32U4 with 28kB of memory available to the user. An RNXV WiFly module is interfaced to the robot using appropriate electronics for wireless communication with a desktop computer. The desktop computer has a 64-bit Windows 11 operating system with installed RAM of 40 GB and an Intel i7-8700 CPU with clock speed of 3.20 GHz. The desktop computer is also interfaced with OptiTrack motion capture system [25], which provides the pose measurements of the robot, with mean error in position of 5.4 mm. The sampling rate of the motion capture system is 240 frames per second, which translates to a sampling period of about 4.1ms. The motion capture system communicates the measurements over a wired single hop network connection and the latency in this communication could be up to 1ms. The desktop computer monitors the event-triggering rule and also computes the coefficients of ETPC whenever required. This computational latency on the computer depends on the prediction horizon T and integration time step, which could go up to 25ms. After an event occurs and the desktop computer computes the ETPC coefficients, it communicates them with the robot wirelessly. The sum of latency in the wireless network, control loops on the robot and the latency caused by onboard serial communication on the robot is on average between 15ms to 20ms but sometimes could go up to 100 ms.

The design parameters for experiments were chosen so that ETC and ETPC have a similar ε_1^2 ultimate bound on V . In particular, the chosen parameters are $\gamma = 1$, $c_1 = 0.5$, $c_2 = 0.8$, $c_3 = 0.7$, and $\sigma = 0.9$. In our experiments, we use Transmission Control Protocol (TCP) which is an upper layer protocol to the Internet Protocol (IP). The size of each IP packet is fixed at 64 Bytes, in which 46 Bytes are reserved for data [26]. For ETC, TTC1 and TTC2, the size of payload (actual intended message) is 4 Bytes while it is 16 Bytes for ETPC. A packet for transmission is constructed by padding the actual payload to achieve the packet sizes required by the protocol. Thus, in comparison to ETC, TTC1, and TTC2, ETPC communicates a lot more information in a single packet less often without affecting communication overheads.

For each path shown in Figure 1, two initial pose errors were considered for each path and for each initial pose error and each algorithm, 10 experiments were conducted. The specific initial pose errors, in (m,m,radians), were chosen as $(0,0,0)$, $(1,0.2,1.57)$ for Path 1; $(0,0,0)$, $(0.2,0.2,1.57)$ for Path 2; $(0,0,0)$, $(0,-0.8,0)$ for Path 3; and $(0,0,0)$,

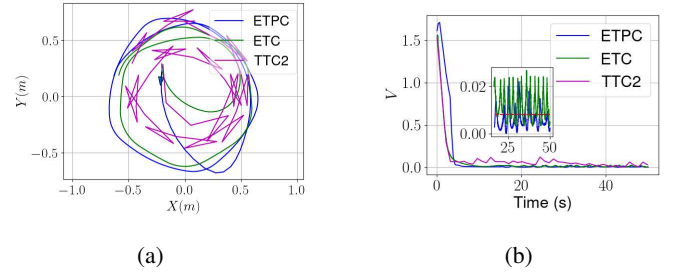


Fig. 6: Results of an experiment of robot tracking the reference trajectory that generates Path 1. (a) Path traced by the robot and (b) the evolution of the Lyapunov function under different algorithms.

$(-0.05, -0.5, -0.02)$ for Path 4.

Figure 6a shows the paths traced by ETC, ETPC and TTC2 for Path 1. It is seen that the robot eventually starts tracking the path with ETC and ETPC algorithms as seen by the corresponding decrease in Lyapunov function as shown in Figure 6b, with V eventually staying within an ultimate bound. For TTC2, we see that the ultimate bound on V is much higher than for ETC and ETPC and the tracking behaviour is not good. Note that due to the unmodeled high computational and communication latency as well as other disturbances and modeling errors, the ultimate bound of V for ETC and ETPC are also higher than the designed ε^2 ,

Figure 7a shows the number of steady state events for all paths. It is observed that the median of N_s for ETPC is reduced by 45% in comparison to median of N_s for ETC.

Similarly, in transient period, the median of N_t for ETPC is reduced by 80.4% in comparison to the median of N_t for ETC as seen in Figure 7b.

Thus, we conclude that in both transient and steady state, our algorithm has fewer number of events. Figure 7c shows the convergence time to ε^2 bound for all algorithms. We see that, in all cases, ETC and ETPC have lower convergence times in comparison to TTC even when outliers are considered. The convergence times for ETC are slightly better than those of ETPC. We also observe that the ultimate bound as seen in Figure 7d is much lower for ETC and ETPC than for TTC and somewhat similar for ETC and ETPC. Recall that in experiments, there are several unmodeled features such as sampling rate for the motion capture, measurement latency, error in obtained pose information, computation times for solving the optimization problem (9), communication delays and latency, delay introduced by onboard serial communication on robot, and environmental conditions such as slip and non-uniform surface friction. Thus, the true ultimate bound for V is usually higher than ε^2 for all the algorithms. From the suite of simulations and experiments, we can conclude that our algorithm has fewer number of events than ETC while ensuring similar tracking behaviour. Compared to TTC with a similar average transmission frequency, the performance of ETC and ETPC are far superior.

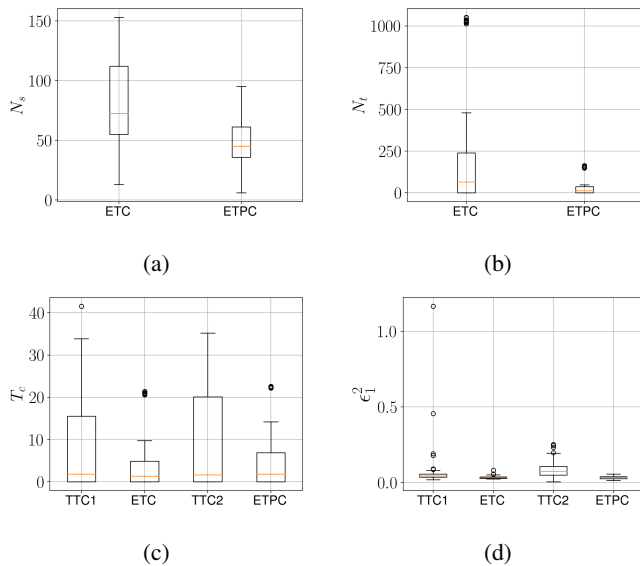


Fig. 7: Results of practical experiments for all the paths and all algorithms. (a) Number of events in steady state, (b) number of events in transient period, (c) time for V to converge to ϵ^2 bound, (d) ultimate bound of V .

VI. CONCLUSION

In this paper, we proposed an event-triggered polynomial control method for trajectory tracking of unicycle robots where the reference trajectory is modeled as the solution of a reference system with unicycle dynamics. In this control method, between two consecutive events, each control input to the robot is a polynomial whose coefficients are chosen to minimize the error in approximating a continuous-time control signal. At each event, the coefficients of the polynomial control input are updated and communicated to the actuator. We designed an event-triggering rule that guarantees uniform ultimate boundedness of tracking error and non-zero behavior of inter-event times. The proposed method works best in cases where communication is significantly more costly than computation. We illustrated the results through numerical simulations and experiments. We also showed that the number of events generated by the proposed controller is significantly less compared to a time-triggered controller and an event-triggered controller based on zero-order hold, while guaranteeing similar tracking performance. Future work includes control under input disturbances, time delays, quantization of the parameters and multi-robot control.

REFERENCES

- [1] P. Tabuada, "Event-triggered real-time scheduling of stabilizing control tasks," *IEEE Transactions on Automatic Control*, vol. 52, no. 9, pp. 1680–1685, 2007.
- [2] W. P. M. H. Heemels, K. H. Johansson, and P. Tabuada, "An introduction to event-triggered and self-triggered control," in *IEEE Conference on Decision and Control (CDC)*, 2012, pp. 3270–3285.
- [3] M. Lemmon, "Event-triggered feedback in control, estimation, and optimization," in *Networked control systems*. Springer, 2010, pp. 293–358.
- [4] D. Tolić and S. Hirche, *Networked control systems with intermittent feedback*. CRC Press, 2017.
- [5] D. Hercog, *Communication protocols: principles, methods and specifications*. Springer, 2020.
- [6] P. Tallapragada and N. Chopra, "On event triggered tracking for nonlinear systems," *IEEE Transactions on Automatic Control*, vol. 58, no. 9, pp. 2343–2348, 2013.
- [7] R. Postoyan, M. C. Bragagnolo, E. Galbrun, J. Daafouz, D. Nešić, and E. B. Castelan, "Event-triggered tracking control of unicycle mobile robots," *Automatica*, vol. 52, pp. 302–308, 2015.
- [8] C. Xie, Y. Fan, and J. Qiu, "Event-based tracking control for nonholonomic mobile robots," *Nonlinear Analysis: Hybrid Systems*, vol. 38, p. 100945, 2020.
- [9] C. Santos, F. Espinosa, E. Santiso, and D. Gualda, "Lyapunov self-triggered controller for nonlinear trajectory tracking of unicycle-type robot," *International Journal of Control, Automation and Systems*, vol. 18, no. 7, pp. 1829–1838, 2020.
- [10] C. Santos, M. Mazo Jr, and F. Espinosa, "Adaptive self-triggered control of a remotely operated p3-dx robot: Simulation and experimentation," *Robotics and Autonomous Systems*, vol. 62, no. 6, pp. 847–854, 2014.
- [11] K. G. Vamvoudakis, A. Mojjoodi, and H. Ferraz, "Event-triggered optimal tracking control of nonlinear systems," *International Journal of Robust and Nonlinear Control*, vol. 27, no. 4, pp. 598–619, 2017.
- [12] Q. Cao, Z. Sun, Y. Xia, and L. Dai, "Self-triggered MPC for trajectory tracking of unicycle-type robots with external disturbance," *Journal of the Franklin Institute*, vol. 356, no. 11, pp. 5593–5610, 2019.
- [13] P. Gao, G. Wang, Y. Ji, Q. Li, J. Zhang, Y. Shen, and P. Li, "Event-triggered tracking control scheme for quadrotors with external disturbances: Theory and validations," in *2022 International Conference on Robotics and Automation (ICRA)*, 2022, pp. 8929–8935.
- [14] P. Zhang, T. Liu, and Z.-P. Jiang, "Tracking control of unicycle mobile robots with event-triggered and self-triggered feedback," *IEEE Transactions on Automatic Control*, vol. 68, no. 4, pp. 2261–2276, 2023.
- [15] E. García and P. Antsaklis, "Model-based event-triggered control for systems with quantization and time-varying network delays," *IEEE Transactions on Automatic Control*, vol. 58, pp. 422–434, 02 2013.
- [16] W. Heemels and M. Donkers, "Model-based periodic event-triggered control for linear systems," *Automatica*, vol. 49, no. 3, pp. 698–711, 2013.
- [17] H. Zhang, D. Yue, X. Yin, and J. Chen, "Adaptive model-based event-triggered control of networked control system with external disturbance," *IET Control Theory & Applications*, vol. 10, no. 15, pp. 1956–1962, 2016.
- [18] L. Zhang, J. Sun, and Q. Yang, "Distributed model-based event-triggered leader–follower consensus control for linear continuous-time multiagent systems," *IEEE Transactions on Systems, Man, and Cybernetics: Systems*, vol. 51, no. 10, pp. 6457–6465, 2021.
- [19] B. Demirel, V. Gupta, D. E. Quevedo, and M. Johansson, "On the trade-off between communication and control cost in event-triggered dead-beat control," *IEEE Transactions on Automatic Control*, vol. 62, no. 6, pp. 2973–2980, 2017.
- [20] A. Li and J. Sun, "Resource limited event-triggered model predictive control for continuous-time nonlinear systems based on first-order hold," *Nonlinear Analysis: Hybrid Systems*, vol. 47, p. 101273, 2023.
- [21] K. Hashimoto, S. Adachi, and D. V. Dimarogonas, "Self-triggered model predictive control for nonlinear input-affine dynamical systems via adaptive control samples selection," *IEEE Transactions on Automatic Control*, vol. 62, no. 1, pp. 177–189, 2017.
- [22] A. Rajan and P. Tallapragada, "Event-triggered parameterized control for stabilization of linear systems," *Accepted at 62nd IEEE Conference on Decision and Control (CDC)*, 2023.
- [23] Z.-P. Jiang and H. Nijmeijer, "Tracking control of mobile robots: A case study in backstepping," *Automatica*, vol. 33, no. 7, p. 1393 – 1399, 1997.
- [24] "3pi+ 32U4 Robot - Turtle Edition (75:1 LP Motors), Assembled," <https://www.pololu.com/product/3738>, accessed: 2023-08-12.
- [25] "NaturalPoint, "Motion Capture Systems -OptiTrack Webpage."," <https://optitrack.com>, accessed: 2023-08-12.
- [26] C. Hornig, "A standard for the transmission of ip datagrams over ethernet networks," Internet Requests for Comments, Symbolics Cambridge Research Center, RFC 894, 4 1984. [Online]. Available: <https://www.rfc-editor.org/rfc/rfc894.txt>